

# Proximal tubular handling of phosphate: A molecular perspective

IC Forster<sup>1,2</sup>, N Hernando<sup>1,2</sup>, J Biber<sup>1</sup> and H Murer<sup>1</sup>

<sup>1</sup>Institute of Physiology and ZIHP, Zurich Center for Integrative Human Physiology, University of Zurich, Zurich, Switzerland

Members of the SLC34 gene family of solute carriers encode for three Na<sup>+</sup>-dependent phosphate (P<sub>i</sub>) cotransporter proteins, two of which (NaPi-IIa/SLC34A1 and NaPi-IIc/SLC34A3) control renal reabsorption of P<sub>i</sub> in the proximal tubule of mammals, whereas NaPi-IIb/SLC34A2 mediates P<sub>i</sub> transport in organs other than the kidney. The P<sub>i</sub> transport mechanism has been extensively studied in heterologous expression systems and structure–function studies have begun to reveal the intricacies of the transport cycle at the molecular level using techniques such as cysteine scanning mutagenesis, and voltage clamp fluorometry. Moreover, sequence differences between the three types of cotransporters have been exploited to obtain information about the molecular determinants of hormonal sensitivity and electrogenicity. Renal handling of P<sub>i</sub> is regulated by hormonal and non-hormonal factors. Changes in urinary excretion of P<sub>i</sub> are almost invariably mirrored by changes in the apical expression of NaPi-IIa and NaPi-IIc in proximal tubules. Therefore, understanding the mechanisms that control the apical expression of NaPi-IIa and NaPi-IIc as well as their functional properties is critical to understanding how an organism achieves P<sub>i</sub> homeostasis.

*Kidney International* (2006) **70**, 1548–1559. doi:10.1038/sj.ki.5001813; published online 6 September 2006

KEYWORDS: electrophysiology; phosphate homeostasis; proximal tubule; renal tubular epithelial cells

Homeostasis of P<sub>i</sub> in higher organisms depends on the coordinated transport of P<sub>i</sub> across intestinal and renal epithelia. Transport of P<sub>i</sub> across the apical membrane is mediated by the three members of the SLC34 family of solute carriers.<sup>1</sup> NaPi-IIa (SLC34A1) and NaPi-IIc (SLC34A3) are specifically expressed in the brush border membrane (BBM) of renal proximal tubules. NaPi-IIb (SLC34A2) has a broader pattern of expression and it is highly abundant in the BBM of small intestine. In both epithelia, the basolateral exit of P<sub>i</sub> is mediated by a transporter that remains unidentified. In the proximal tubule it has been proposed that a Na<sup>+</sup>-dependent electroneutral anion exchanger is at least partially responsible for P<sub>i</sub> exit.<sup>2</sup>

NaPi-IIa and NaPi-IIc mediate the reabsorption of P<sub>i</sub> from the primary urine by using the free energy provided by the electrochemical gradient for Na<sup>+</sup>. NaPi-IIa is electrogenic and transports divalent P<sub>i</sub> preferentially. It functions with a strict Na<sup>+</sup>:P<sub>i</sub> stoichiometry of 3:1, which results in the net inward movement of one positive charge per cotransport cycle.<sup>3</sup> NaPi-IIc, in contrast, is electroneutral and exhibits a 2:1 stoichiometry<sup>4,5</sup> (Figure 1). In mice, NaPi-IIa is the protein mainly responsible for P<sub>i</sub> reabsorption in the adult kidney, whereas NaPi-IIc appears to be more important in weaning animals. Indeed, the phenotype of NaPi-IIa knockout mice first suggested that this cotransporter is responsible for the bulk of renal P<sub>i</sub> reabsorption with a very small percentage potentially attributed to NaPi-IIc.<sup>6</sup> However, recent data indicate that in humans, NaPi-IIc may have a previously unpredicted importance. The expression of NaPi-IIa and NaPi-IIc is regulated to adapt the renal reabsorption of P<sub>i</sub> to the organism needs. Thus, the phosphaturic effect associated with parathyroid hormone (PTH) is due to the membrane retrieval of both cotransporters, whereas in conditions of P<sub>i</sub> deprivation their expression is increased.<sup>4,7–9</sup>

The following sections summarize our present state of knowledge of the regulatory and pathophysiological roles of NaPi-IIa in renal P<sub>i</sub> handling as well as its mechanism and structure–function relations.

## REGULATION OF NaPi-IIa EXPRESSION

Many hormonal and non-hormonal factors regulate renal reabsorption of P<sub>i</sub> (for review, see Murer *et al.*<sup>10</sup>). The effect of PTH and dietary P<sub>i</sub> on NaPi-IIa has been the subject of detailed investigation. These studies suggest that NaPi-IIa

**Correspondence:** IC Forster or N Hernando, Institute of Physiology, Winterthurerstrasse 190, Zurich CH-8057, Switzerland.

E-mails: iforster@access.unizh.ch; hernando@physiol.unizh.ch

<sup>2</sup>These authors contributed equally to this work

Received 28 June 2006; revised 12 July 2006; accepted 18 July 2006; published online 6 September 2006

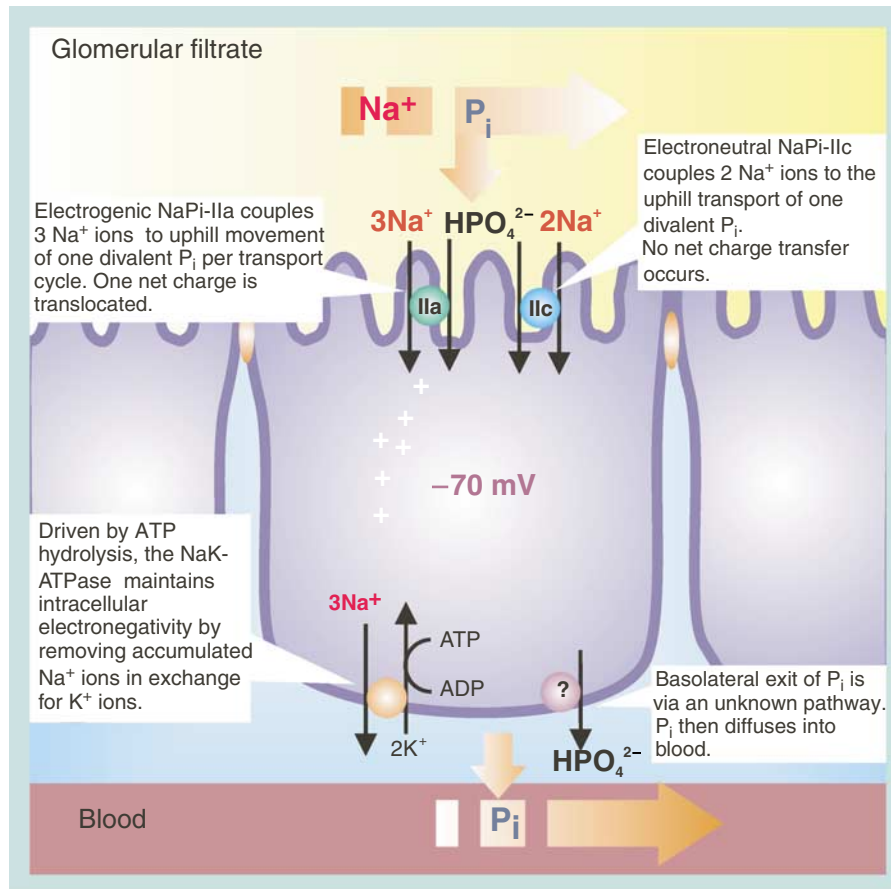


**Figure 1 | Energetics of P<sub>i</sub> reabsorption.** In the BBM of proximal tubule epithelia, two Na<sup>+</sup>-coupled transporters, designated as NaPi-IIa and NaPi-IIc, mediate apical uptake of P<sub>i</sub> from the glomerular filtrate. Both are secondary active and drive P<sub>i</sub> inward using the electrochemical free energy difference across the membrane for Na<sup>+</sup> ions. NaPi-IIa is electrogenic and NaPi-IIc is electroneutral. With a typical transmembrane Na<sup>+</sup> concentration ratio of 10:1, the theoretical P<sub>i</sub> concentrating capacity of NaPi-IIc is ~100:1, whereas that for NaPi-IIa is ~10 000:1 because of its 3:1 Na<sup>+</sup>:P<sub>i</sub> stoichiometry and the additional driving force contributed by the transmembrane potential difference.

regulation depends on its shuttling to/from the BBM. This contrasts with many other transporters, which activity is modulated by modification of the transport protein itself (e.g. phosphorylation, dimerization etc). This means that the body's requirements for a higher P<sub>i</sub> reabsorption (i.e. after low P<sub>i</sub>-diet) are met by increasing the expression of NaPi-IIa<sup>7,11,12</sup> and NaPi-IIc<sup>4</sup> at the BBM. For NaPi-IIa, acute upregulation is independent of changes in transcription or translation. Therefore, the increased expression of NaPi-IIa must be owing to either the stabilization of the transporter at the BBM or to an increased rate of insertion at the membrane. Experimental data supports this dual mechanism. Thus, dietary-induced upregulation depends on the presence of scaffolding proteins,<sup>13</sup> suggesting a stabilization action, and on the microtubule network,<sup>11</sup> suggesting an increased rate of insertion. This latter mechanism requires the presence of an intracellular pool of NaPi-IIa ready to be shuttled to the membrane. Immunostainings of kidneys from rats fed acutely a low P<sub>i</sub>-diet have indeed revealed the presence of NaPi-IIa in the Golgi apparatus, although this pool is not detected with all immunostaining protocols.<sup>11</sup>

In contrast, reduced reabsorption of P<sub>i</sub> (i.e. upon PTH release or high P<sub>i</sub>-diet) is achieved via downregulation of NaPi-IIa<sup>8,11,14</sup> and NaPi-IIc<sup>9</sup> at the BBM. PTH-induced downregulation of NaPi-IIa has been extensively studied and the identifiable steps are summarized in Figure 2. Because endocytosed cotransporters do not recycle to the BBM but instead are degraded in lysosomes, recovery of NaPi-IIa basal levels upon PTH removal depends on *de novo* synthesis. It is therefore clear that apical retention/removal of NaPi-IIa must be a regulated process, beyond the control of protein turnover. We will now describe in detail the steps summarized in Figure 2, integrating what is known about the mechanisms that regulate NaPi-IIa expression with the role of protein complexes.

#### Regulation of apical expression (step 1)

Apical expression of NaPi-IIa is dependent on its last three residues (TRL, see Figure 4a). Truncation of these residues leads to intracellular accumulation of the cotransporter, suggesting an impaired sorting and/or stability of the mutated protein.<sup>15</sup> The TRL sequence represents a PDZ

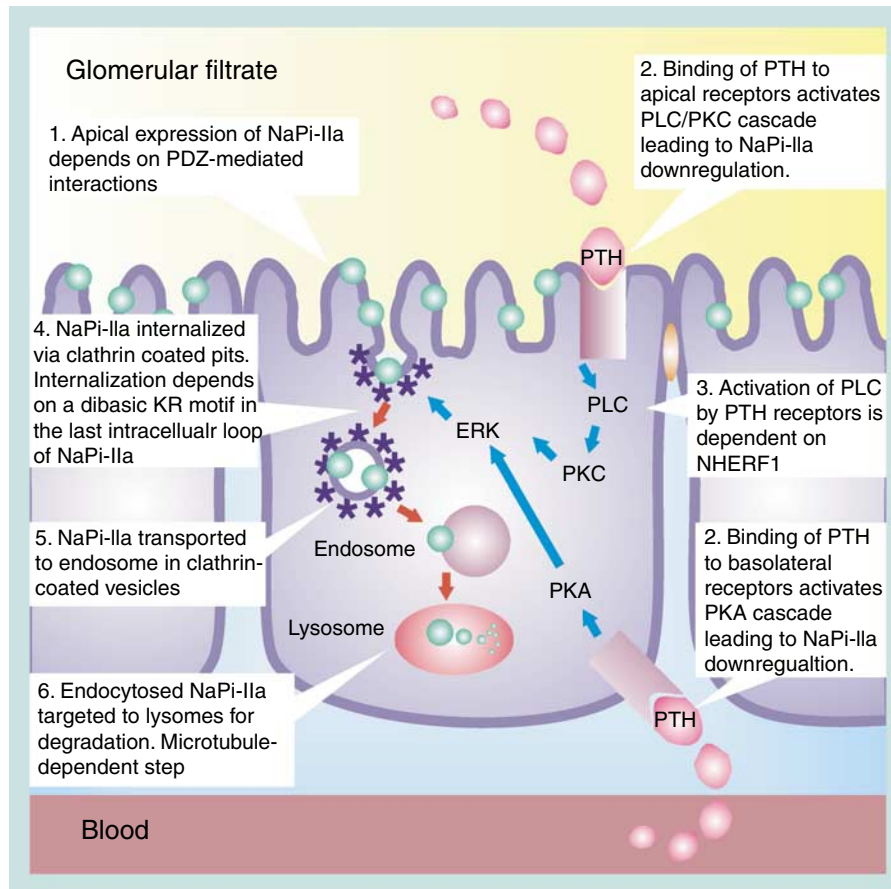


**Figure 2 | The downregulation of NaPi-IIa.** Schematic representation of the sequence of steps involved in PTH-induced downregulation of NaPi-IIa in an epithelial proximal tubule cell. Apical and basolateral membranes are separated by tight junctions (orange), to establish two compartments for hormonal access.

(PSD-95, Discs-large and ZO-1) binding motif that interacts with several PDZ proteins.<sup>16,17</sup> PDZ domains, first described in the early 1990s, comprise 80–100 residues distributed in six  $\beta$  strands and two  $\alpha$  helices. They bind to the carboxyl-terminal tail (PDZ-binding motif) of the corresponding ligand (for review, see Nourry *et al.*<sup>18</sup>). A conserved sequence between the  $\beta$ A and  $\beta$ B strands of the PDZ domain (GLGF) provides a hydrophobic pocket for ligand binding. Among the PDZ proteins that interact with NaPi-IIa are the Na/H-exchanger regulatory factors NHERF1 (EBP50) and NHERF2 (E3KARP) as well as PDZK1 (NHERF3), PDZK2 (IKEPP, NHERF4), and Shank2E.<sup>16,17</sup>

*NHERF1* and *NHERF2* are two related proteins each containing two PDZ domains and a C-terminal Merlin-Ezrin-Radixin-Moesin-binding domain.<sup>19–21</sup> They are expressed in the apical/subapical domain of murine proximal tubules, respectively.<sup>16,22</sup> NaPi-IIa binds to the first PDZ domain on both proteins.<sup>16</sup> Renal proximal cells (opossum kidney cells) transfected with dominant-negative NHERF1 constructs<sup>23</sup> and young NHERF1<sup>-/-</sup> animals<sup>24</sup> show a reduced amount of NaPi-IIa at the BBM. In animals, this reduction associates with urinary loss of P<sub>i</sub>, a phenotype that reverts with age.<sup>25</sup> These findings suggest that NHERF1 contributes to stabilize

NaPi-IIa at the BBM. This stabilization depends on the Merlin-Ezrin-Radixin-Moesin-binding domain,<sup>23</sup> which mediates binding to the actin-associated protein Ezrin. In contrast to the effect on NaPi-IIa, deficiency in NHERF1 does not affect the expression of NHE3.<sup>24</sup>

*PDZK1* and *PDZK2* are related proteins, also expressed in murine proximal tubules, each containing four PDZ domains. In both cases, NaPi-IIa binds to the third PDZ domain.<sup>16,26</sup> Opossum kidney cells transfected with a dominant-negative PDZK1 construct show reduced levels of NaPi-IIa at the BBM.<sup>23</sup> Although NaPi-IIa expression is unaffected in normally fed PDZK1<sup>-/-</sup> mice, its abundance decreases when the animals are fed a high P<sub>i</sub>-diet.<sup>27</sup> Thus, in extreme dietary conditions PDZK1 may contribute to stabilize NaPi-IIa at the BBM.

*Shank2E* is an epithelial-specific isoform of Shank2. The three members of the Shank family share a similar domain structure consisting of six N-terminal ankyrin repeats followed by an SH3 domain, a PDZ domain, and a proline-rich region.<sup>28</sup> In rats, Shank2E is expressed at the BBM of proximal tubules and, as for the other PDZ proteins, association with NaPi-IIa requires the C-terminal TRL motif of the cotransporter.<sup>17</sup> Shank2 can bind dynamin,<sup>29</sup> a

guanosine triphosphatase that mediates fission of endocytic vesicles.<sup>30</sup> Thus, Shank2E may connect NaPi-IIa with the endocytic machinery.

### PTH signaling (steps 2–4)

In the proximal tubule, PTH binds to apical and basolateral receptors. Stimulation of either receptor leads to an increase in urinary excretion of  $P_i$  as consequence of the reduction of NaPi-IIa in the BBM.<sup>31</sup> Apical application of PTH to isolated proximal tubules activates preferentially the phospholipase C/protein kinase C (PKC) pathway, whereas basolateral application leads to activation of cyclic adenosine monophosphate (cAMP)/protein kinase A (PKA) signaling.<sup>31</sup> The molecular explanation for this dual response may relay on the presence (apical) or absence (basolateral) of NHERF. Thus, it has been shown that NHERF associates with both the PTH receptor and the phospholipase C $\beta$ 1.<sup>32</sup> The consequence of this intermolecular association is the preferential activation of phospholipase C upon binding of PTH to apical receptors. In accordance with this mechanism, both 1–34 PTH (a fragment that activates PKA and PKC) and 3–34 PTH (a fragment that activates only PKC) fail to activate phospholipase C in kidney slices from NHERF1<sup>-/-</sup> mice.<sup>33</sup> Despite the heterogeneity of their initial steps, apical, and basolateral PTH receptors use common downstream effectors. Mitogen-activated protein kinase-kinase 1/2 inhibitors partially or fully prevent the effect of both cascades, suggesting that the PKC and PKA pathways coactivate extracellular signal-regulated protein kinase 1/2.<sup>34</sup> Interestingly, NHERF1 plays a very different role in the regulation of NHE3, where acts as a scaffold for PKA via association with the cAMP-kinase associated protein Ezrin.<sup>35</sup> Then, PKA phosphorylates (and inhibits) NHE3 without initial changes in the expression of NHE3 in the BBM.<sup>36</sup> cAMP-induced inhibition of NHE3 can be reproduced with cAMP analogs that activate exchange protein directly activated by cAMP (EPAC1), whereas NaPi-IIa is downregulated by PKA- but not by EPAC1-activating analogs.<sup>37</sup>

### PTH-induced endocytosis of NaPi-IIa (steps 5 and 6)

Binding of PTH leads to the axial movement of NaPi-IIa along the microvilli and finally to its endocytosis from the microvillar clefts.<sup>38,39</sup> NaPi-IIa colocalizes with insulin upon PTH administration, suggesting its internalization via receptor-mediated endocytosis.<sup>40</sup> This is further supported by the finding that NaPi-IIa endocytosis is prevented in mice with kidney-specific megalin deficiency and in receptor-associate-protein-deficient mice.<sup>41</sup> The immunostainings shown in Figure 3 illustrate the route followed by NaPi-IIa in response to PTH.<sup>40</sup> Endocytosis takes place via clathrin-coated pits and it is detected shortly upon PTH administration. Later on, NaPi-IIa is observed in clathrin-coated pits and in endosomes (early endosome-associated protein 1 (EEA1) positive). Finally, the cotransporter is targeted to late endosomes/lysosomes (lgp120 positive). Endocytosis associates with microtubule rearrangement, owing to the formation

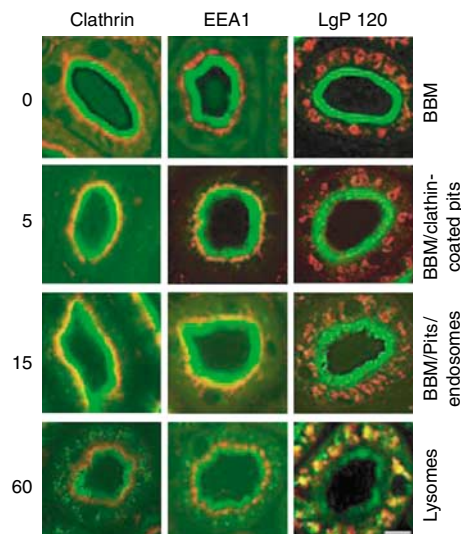


**Figure 3 | Immunohistochemical evidence for NaPi-IIa down-regulation.** Immunofluorescence of kidney slices incubated in the absence or presence (5, 15, and 60 min) of PTH. Samples were co-stained with antibodies against NaPi-IIa (green) and either clathrin, EEA1, or lgp120 (red) antibodies.

of apical to basolateral oriented bundles.<sup>42</sup> Prevention of microtubular rearrangement or microtubular depolymerization causes the delay of intracellular depletion of NaPi-IIa (i.e. lysosomal degradation), although it does not affect its downregulation (i.e. endocytosis).

Clathrin-mediated internalization of many proteins depends on discrete intracellular sequences, among them tyrosine (Y)- and dileucine (LL)-based motifs. These motifs link the protein to be endocytosed to the adaptor protein AP2 which in turn binds to clathrin (for review, see Robinson<sup>43</sup>). AP2 is a heterotetramer consisting of  $\alpha$ ,  $\beta$ 2,  $\mu$ 2, and  $\sigma$ 2 subunits. Y-based motifs bind to the  $\mu$  subunit whereas LL-based motifs interact with the  $\beta$  subunit. NaPi-IIa contains several putative Y- or LL-motifs (GY<sub>402</sub>FAM, Y<sub>509</sub>RWF, LL<sub>101</sub>, LL<sub>374</sub>, and LI<sub>590</sub>) and two diacidic sequences (EE<sub>81</sub> and EE<sub>616</sub>) that can control lysosomal targeting. Mutations of these motifs did not affect the PTH-induced retrieval of NaPi-IIa.<sup>44</sup> Instead, a dibasic sequence (KR) within the last intracellular loop (Figure 4a) is required for PTH sensitivity.<sup>45</sup> These two positively charged residues are replaced by uncharged residues (NI) in the PTH-insensitive NaPi-IIb isoform. Swapping the specific residues inverts the PTH sensitivity of the protein. The KR-containing loop, but not a mutant with the KR sequence replaced by NI, interacts with PEX19.<sup>46</sup> In opossum kidney cells, NaPi-IIa endocytosis is accelerated upon transfection of PEX19, suggesting a role of this protein in the internalization of the cotransporter.<sup>46</sup>

NHERF1 and PDZK1 remain attached to the BBM upon PTH administration; Deliot *et al.*,<sup>47</sup> in preparation. This suggests the disassembly of protein complexes before internalization of NaPi-IIa. In opossum kidney cells, the amount of NaPi-IIa that coimmunoprecipitates with

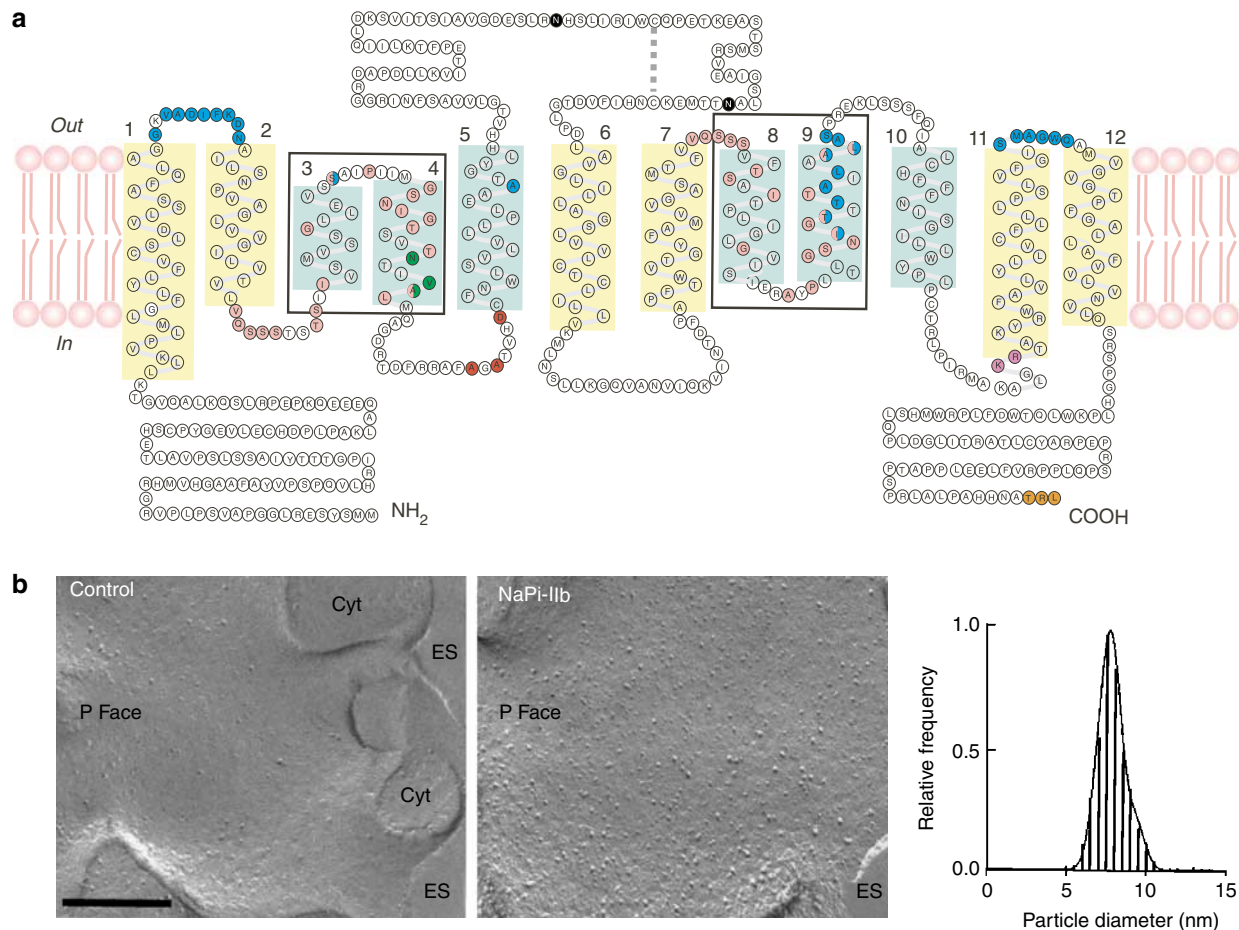


**Figure 4 | The NaPi-II protein.** (a) *Topological map of NaPi-IIa.* This scheme is based on prediction algorithms and experimental data. The NaPi-IIa monomer comprises twelve  $\alpha$ -helical segments, four of which (yellow) have been confirmed by *in vitro* translation assays to span the membrane.<sup>67</sup> substituted cysteine accessibility method (see text) has revealed sites accessible from the external,<sup>69,70,72–74</sup> (blue) and internal<sup>71</sup> (green) sides of the membrane, respectively. Two reentrant regions in each half of the protein, which comprise putative  $\alpha$ -helical segments 3–4 and 8–9 (boxed) and the preceding linkers, contain identical residues (pink). They are proposed to form the substrate translocation pathway.<sup>75</sup> A disulfide bridge in the large extracellular loop links the two halves of the protein. Regulatory sites include the K-R motif<sup>45</sup> (orange), important for PTH-induced internalization, located at the cytosolic end of  $\alpha$ -helical domain 11<sup>15</sup> and the triglyceride-rich lipoproteins motif (violet) at the end of the C-terminal tail, involved in PDZ interactions.<sup>15</sup> The large extracellular linker region contains two N-glycosylation sites (black). Three sites were found critical for NaPi-IIa electrogenicity in the linker between  $\alpha$ -helical segments 4–5 (red).<sup>5</sup> (b) *Evidence for NaPi-II dimers in the plasma membrane.* Freeze fracture micrographs of the P face of the oocyte plasma membrane show a low density of endogenous particles in a control oocyte (left) and an increased particle density in an oocyte expressing the flounder renal/intestinal NaPi-IIb (center). Scale bar for both images: 200 nm. P Face = protoplasmic face, ES = extracellular space; Cyt = cytosol. Statistical analysis of particle diameter (right) suggests a homodimeric complex for NaPi-IIb proteins based on freeze-fracture analysis of other membrane proteins.<sup>86</sup> Images and analysis courtesy of S. Eskandari, Biological Sciences Department, California State Polytechnic University, Pomona, CA, USA.

NHERF1 is reduced upon PTH treatment.<sup>47</sup> Thus, PTH may negatively regulate the association between NaPi-IIa and NHERF1/PDZK1. PDZ-based interactions can be regulated by phosphorylation of either the PDZ-binding motif or the corresponding PDZ-domain. Studies using cell culture models have demonstrated that NHERF1 is constitutively phosphorylated, and the residues responsible for constitutive and regulated phosphorylation have been identified.<sup>48–50</sup> NHERF1 is also constitutively phosphorylated in mouse kidney.<sup>47</sup> Moreover, PTH, or pharmacological activation of PKA and PKC induces phosphorylation of NHERF1, but not of NaPi-IIa. PDZK1 is also constitutively phosphorylated in kidney, and similar to NHERF1, PTH, or activation of

kinases, leads to an increase in its phosphorylation state (N. Déliot, N. Hernando, unpublished experiments). Thus, we can hypothesize that phosphorylation of the PDZ-proteins destabilizes their association with NaPi-IIa. According to a recent report, PDZK1 is phosphorylated by PKA in Ser<sub>509</sub> and this modification is required for upregulation of the scavenger receptor class B type I.<sup>51</sup>

Like PTH, a high  $P_i$ -diet also induces downregulation of NaPi-IIa.<sup>7,8,11,12</sup> Although this process has not been studied in the same detail as the PTH effect, endocytosed cotransporters are also degraded in lysosomes.<sup>8,12</sup> Thus, PTH and  $P_i$ -diet may lead to similar cellular responses. Expression of NHERF1 and PDZK1 remain unaffected upon

changes in dietary  $P_i$ . However, Shank2E is endocytosed in response to high  $P_i$ -diet.<sup>17</sup> As mentioned above, Shank2 can bind dynamin II<sup>29</sup> and therefore it could participate in the linkage of NaPi-IIa with the endocytic machinery. In this regard, Shank2E was shown to have a high rate of degradation even under low  $P_i$ -diet, suggesting its constitutive association with the endocytic process.

#### NaPi-II COTRANSPORTERS AND HUMAN DISEASE

Several human disorders associate with renal  $P_i$  wasting. The best characterized are X-linked hypophosphatemia, for which two animal models (*Hyp* and *Gy* mice) are available, autosomal dominant hypophosphatemic rickets, and hereditary hypophosphatemic rickets with hypercalciuria (HHRH) (for review, see Tenenhouse and Murer<sup>52</sup>).

*Hyp* and *Gy* mice show a reduced expression of NaPi-IIa and NaPi-IIc.<sup>53,54</sup> However, the primary defect does not reside on the cotransporter genes. Instead, reduction of NaPi-II is due to phosphate regulating gene with homology to endopeptidases on the X chromosome (PHEX), a circulating factor secreted by osteoblasts.<sup>55</sup> PHEX has some homology with metallopeptidases and it has been proposed that its role is to degrade a phosphaturic factor which nature remains controversial.

The gene responsible for autosomal dominant hypophosphatemic rickets has also been identified.<sup>56</sup> It encodes fibroblast growth factor-23 (FGF23), which is proteolytically cleaved at a furin site. In mice, infusion of FGF23 leads to hyperphosphaturia owing to a reduction of NaPi-IIa in the proximal BBM<sup>57,58</sup> whereas FGF23 deficient mice show hyperphosphatemia.<sup>59</sup> Although it was proposed that FGF23 may be a substrate of PHEX this remains to be further confirmed.

HHRH is an autosomal recessive hypophosphatemic disorder. Unlike other forms of hypophosphatemia, HHRH associates with elevated levels of 1,25-dihydroxyvitamin D which lead to increased intestinal reabsorption of calcium and hypercalciuria.<sup>60</sup> Because this phenotype is similar to the one presented in NaPi-IIa-deficient mice<sup>6</sup> it was postulated that mutations in NaPi-IIa could be responsible for HHRH. Several single nucleotide polymorphisms on the NaPi-IIa gene (*NPT2* or *SLC34A1*) were detected in families affected by this syndrome; however, no mutations predicted to affect the protein were found.<sup>61</sup> Heterozygous mutations on NaPi-IIa have been reported in two patients with hypophosphatemia associated with urolithiasis or bone demineralization<sup>62</sup> and initial reports suggested that the mutations affected the apparent affinity for  $P_i$  and membrane targeting. However, an extensive kinetic analysis of those mutants performed in our laboratory<sup>63</sup> as well as the phenotype of the heterozygous NaPi-IIa<sup>+/-</sup> mice<sup>6</sup> do not support the concept of these heterozygous mutations being responsible for the human disease. Recently, several groups reported homozygous mutations in *SLC34A3*, the gene coding NaPi-IIc, in patients with HHRH.<sup>64,65</sup> Based on mice data, NaPi-IIc is predicted to mediate not more than 30% of proximal reabsorption of  $P_i$ .

However, the above findings suggest a more critical role of this transporter in the human kidney.

#### MOLECULAR MECHANISM OF $P_i$ COTRANSPORT BY NaPi-IIa

##### The NaPi-IIa protein

Mammalian NaPi-IIa proteins are typically ~640 amino acids long with a glycosylated molecular weight of ~80–90 kDa.<sup>66</sup> The secondary topology (Figure 4a) has been determined from topology prediction algorithms and *in vitro* translation assays,<sup>67</sup> epitope tagging studies,<sup>68</sup> and cysteine scanning assays.<sup>69–74</sup> The current model comprises 12  $\alpha$ -helical segments and a large extracellular loop that contains two N-glycosylation sites with intracellular amino and carboxyl tails. Four of the  $\alpha$ -helical domains are proposed to form two opposed reentrant segments (3, 4 and 8, 9) that are speculated to associate and constitute the transport pathway.<sup>75</sup> Interestingly, these regions contain repeated sequences that are conserved in all eukaryotic NaPi-II isoforms,<sup>71,76</sup> as well as in the bacterial homolog from *Vibrio cholerae*.<sup>77</sup> This strongly suggests a common structure–function motif among  $Na^+$ -driven  $P_i$  cotransporters that has been preserved throughout the course of evolution. One disulfide bridge, in the large extracellular loop, most likely serves to define the tertiary structure and links the two halves of the protein. This bridge has been shown to be essential for functional expression<sup>76</sup> and the two halves have not been successfully expressed individually.<sup>74,78</sup> A second disulfide bridge linking cysteine residues within the hydrophobic core of the protein has also been proposed, although the cysteine pair involved is less certain.<sup>76,79</sup>

Homomultimeric assembly is a feature of channel proteins: the oligomerization can be essential for function as in the case of tetrameric  $K^+$  channels<sup>80</sup> or a structural requirement as in the case of the dimeric  $Cl^-$  channels.<sup>81</sup> Multimeric assemblies of carrier proteins have also been proposed (e.g.<sup>82</sup>Kilic and Rudnick; <sup>83</sup>Eskandari *et al.*) and recently the crystallization of a bacterial glutamate transporter homolog revealed a trimeric assembly.<sup>84</sup> These findings prompt two questions: what is the functional unit of NaPi-II proteins and do they oligomerize *in vivo*? To answer the first question, we performed coexpression experiments with the wild-type (WT) NaPi-IIa and a selectively inhibitable mutant NaPi-IIa, as well as experiments using an engineered concatamer comprising the WT and the same mutant. Our findings established conclusively that the NaPi-IIa protein is a functional monomer.<sup>85</sup> With regard to the second question, compelling evidence has emerged in favor of the dimerization of NaPi-IIa *in situ*: the freeze fracture technique<sup>86</sup> applied to *Xenopus* oocyte membranes containing the flounder renal/intestinal NaPi-IIb revealed membranous particles, with a mean diameter of 7.5 nm that would be consistent with a dimeric assembly of NaPi-IIb proteins (Figure 4b, S Eskandari, personal communication). This conclusion is also supported by evidence from two other approaches: (1) application of the split ubiquitin method to detect protein–protein interactions<sup>87</sup> confirmed that NaPi-IIa can self-associate

*in vitro* and (2) by means of dual tagging, dimerization was documented for NaPi-IIa expressed in *Xenopus* oocytes.<sup>87</sup>

### Transport mechanism

The basic kinetic characteristics of renal proximal tubular Na<sup>+</sup>-P<sub>i</sub> cotransport were determined using BBM vesicles before the identification of the proteins responsible (for review, see Murer *et al.*<sup>66</sup>). With the exception of the issues of electrogenicity and the identification of the preferred species of P<sub>i</sub> cotransported, both of which could not be clearly resolved from these earlier studies alone, the kinetic fingerprint has remained essentially the same after expression cloning and functional characterization of the NaPi-II proteins in heterologous expression systems. Its features are: (1) a strict dependency on external Na<sup>+</sup> as the driving substrate, with an apparent affinity of Na<sup>+</sup> of ~50 mM, (2) a specificity for P<sub>i</sub> as the driven substrate with an apparent affinity of ≤0.1 mM, and (3) a strong dependency on external pH, whereby extracellular acidification diminishes P<sub>i</sub> uptake.

By means of expression cloning, the identification of the NaPi-IIa protein as the principal mediator of Na<sup>+</sup>-coupled P<sub>i</sub> uptake in the mammalian kidney and the expression in *Xenopus* oocytes of different NaPi-IIa isoforms has allowed more detailed kinetic studies to be performed. The first of these documented the electrogenicity of NaPi-IIa.<sup>88</sup> When the membrane potential of a *Xenopus* oocyte overexpressing NaPi-IIa is measured in the presence of Na<sup>+</sup>, application of P<sub>i</sub> causes membrane depolarization, consistent with an inwardly directed net positive charge movement; restoration of the cell resting potential occurs after removal of P<sub>i</sub> (Figure 5a). Moreover, when the membrane potential is fixed to a value in the physiological range (i.e. the oocyte membrane is voltage clamped), P<sub>i</sub> induces inward currents that are membrane potential dependent (Figure 5b). Under the assumption that the electrogenic activity is a direct reflection of the transport activity, these basic findings led to the proposal that the NaPi-IIa protein operates with a Na<sup>+</sup>:P<sub>i</sub> stoichiometry of 3:1 at physiological pH (7.4), where divalent P<sub>i</sub> predominates. However, there was still uncertainty about the selectivity of the transporter for divalent versus monovalent P<sub>i</sub> and the influence of external pH, which itself determines the availability of the P<sub>i</sub> species (e.g.<sup>88,89</sup> Busch *et al.*;<sup>90</sup> Hartmann *et al.*). This issue was resolved unambiguously by simultaneous measurement of net charge transfer and substrate flux on the same oocytes.<sup>3,91</sup> Moreover, these studies confirmed that NaPi-IIa preferentially transports divalent P<sub>i</sub>, independently of the external pH.

Two other properties of electrogenic NaPi-II proteins are presteady-state charge movements and uncoupled leak currents. When challenged by a step change in membrane potential, NaPi-IIa expressing oocytes exhibit nonlinear charge movements, termed presteady-state relaxations, which have been reported for nearly all electrogenic cotransporter systems so far studied (for review, see Forster *et al.*<sup>92</sup>). The detection of these charge movements provided the first, albeit

indirect, evidence that voltage-driven molecular conformational changes occur during the transport process, analogous to the gating currents that precede the opening of voltage gated channels (e.g. Bezanilla<sup>93</sup>). For NaPi-IIa, relaxations are observed in the presence and absence of external Na<sup>+</sup> (Figure 5c): in the latter case, the relaxations are hypothesized to reflect a voltage-driven reorientation of the empty carrier. Such a reorientation would be consistent with an alternating access type model for the uphill movement of solute, in which the protein exposes substrate binding sites either to the external or internal media, but not both at the same time. In the former case, additional charge movement reflects the movement of Na<sup>+</sup> ions to and from their binding sites, located within the transmembrane electric field. The existence of such voltage-dependent processes implies that in addition to substrate activity, membrane potential is also a determinant of the transport rate (Figure 5a-c). Note that the electroneutral NaPi-IIc<sup>4</sup> does not exhibit presteady-state relaxations.<sup>5</sup>

Recent findings have prompted a reconsideration of what distinguishes passive channels from active carriers (e.g. DeFelice<sup>94</sup>): channels can display carrier-like behavior<sup>95</sup> and carriers can display channel-like behavior (e.g. Sonders and Amara<sup>96</sup>). Moreover, the changes at the molecular level that affect the switch between modes can be minor. For electrogenic members of the NaPi-II family, the P<sub>i</sub> transport inhibitor foscarnet (phosphonoformic acid) was shown to inhibit a Na<sup>+</sup>-dependent leak current<sup>97</sup> associated with expression of NaPi-IIa protein in oocytes. Ion-replacement experiments also indicate the involvement of other ions including chloride and suggest a more complex leak pathway than hitherto proposed (I.C. Forster and A. Bacconi, unpublished experiments). Based on studies of mutant NaPi-IIa proteins, the leak and cotransport modes appear to be mutually exclusive,<sup>75</sup> although it has proven experimentally difficult to establish this conclusively for the WT protein. Furthermore, recent studies on the temperature dependency of NaPi-II indicate that the activation energy for the leak mode is more consistent with a carrier type mechanism than that of a channel (A. Bacconi and I. Forster, unpublished experiments). The NaPi-IIa leak current accounts for ~10% of the maximum P<sub>i</sub>-induced current (although some engineered NaPi-IIa mutants exhibit significantly larger leaks (e.g.<sup>71,75</sup> Kohler *et al.*; <sup>72</sup>Virkki *et al.*; and <sup>73,74</sup>Ehnes *et al.*). The physiological significance of these leak currents is yet to be determined and in the proximal tubule with NaPi-IIa operating near V<sub>max</sub> conditions, its leak current is probably inconsequential. It remains to be clarified whether the NaPi-IIa leak current results from translocation of ions by the NaPi-IIa monomer or through a gated pore formed by the putative dimer.

The combined findings of kinetic studies on WT NaPi-IIa proteins have resulted in a kinetic scheme for the transport cycle (Figure 5d). This comprises a sequence of partial reactions in which ordered substrate binding occurs<sup>91,97,98</sup> and is consistent with an alternating access model in which

states 1–4 and 5–8 represent ‘outward’ and ‘inward’ facing conformations, respectively. Recent voltage clamp fluorometry (VCF) studies<sup>99</sup> provide compelling evidence that two  $\text{Na}^+$  ions precede the  $\text{P}_i$  interaction, in contrast to our earlier scheme based on electrophysiological measurements alone, which postulated a single  $\text{Na}^+$  ion interaction.<sup>97</sup> The first

$\text{Na}^+$  interaction (1–2a) is proposed to be electroneutral, which is followed by the movement of a second  $\text{Na}^+$  ion into the transmembrane field that gives rise to the resolvable charge movements. In the absence of  $\text{P}_i$ , the system can cycle via the leak pathway: phosphonoformic acid is thought to compete directly with the  $\text{P}_i$  binding transition and protons

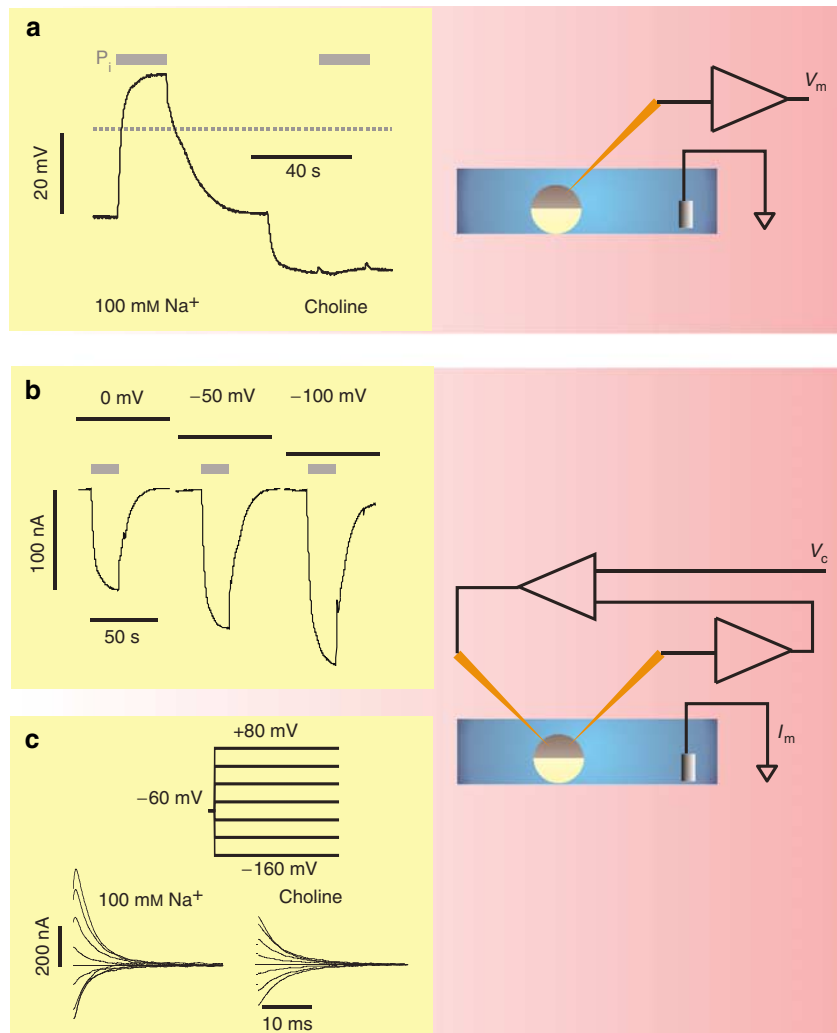


**Figure 5 | NaPi-IIa kinetics.** (a–c) The electrogenicity of NaPi-IIa studied using *Xenopus* oocytes. (a) An oocyte expressing NaPi-IIa is impaled with a microelectrode to measure the transmembrane potential ( $V_m$ ). Application of 1 mM  $\text{P}_i$  in the presence of 100 mM  $\text{Na}^+$  induces membrane depolarization consistent with net translocation of charge. No change in  $V_m$  occurs in the absence of  $\text{Na}^+$ . (b) Impalement of the same oocyte with two intracellular electrodes together with an additional amplifier allows clamping the membrane potential according to an external command ( $V_c$ ) and measurement of the transmembrane current ( $I_m$ ). Application of  $\text{P}_i$  in the presence of  $\text{Na}^+$  induces an inwardly directed current that is also voltage dependent. (c) With the same measurement system as in (b), step changes in  $V_m$  induce transient current relaxations (presteady-state currents) that are also observed in the absence of substrate. In choline they reflect the movement of mobile charges intrinsic to the NaPi-IIa protein; with added 100 mM  $\text{Na}^+$ , additional charge movement reflects movement of  $\text{Na}^+$  ions within the transmembrane field. (d) Kinetic scheme for the NaPi-IIa transport cycle. This comprises an ordered sequence of partial reactions between different conformational states, indicated by the numbers. At least two partial reactions (red) involve charge movement within the transmembrane electric field: the empty carrier (1–8) and  $\text{Na}^+$  binding (2a–2b). They confer voltage dependency to the transport cycle. The partial reactions affected by protons,  $\text{Li}^+$ , and phosphonoformic acid are indicated. Transitions between the postulated inward-facing conformations (5–8) have not been characterized. The leak mode (light blue) involves the translocation of  $\text{Na}^+$  ions before  $\text{P}_i$  binding. In the presence of  $\text{P}_i$ , the complete cotransport cycle (dark blue) is adopted. The translocation of the fully loaded protein (three  $\text{Na}^+$  ions and one divalent  $\text{P}_i$ ) takes place via an electroneutral transition (4–5): we assume that the carrier itself provides one net negative charge, which accounts for the presteady charge movements in choline (c). Finally, on the cytosolic side, we assume that the substrates are released sequentially. The substrate debinding leaves the empty carrier in an unfavorable conformation (for a negative intracellular potential) so that it returns to an outward facing conformation (state 1) for the next cycle. (Figure 5 continued on following page.)



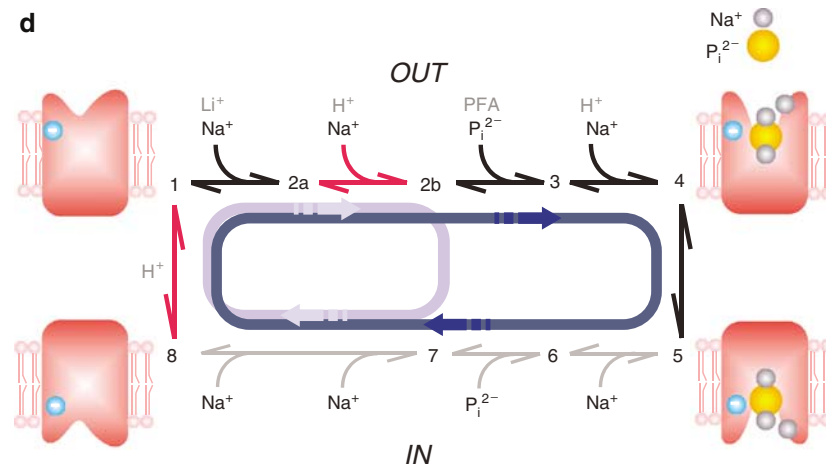


**Figure 5** | Continued

interact at multiple sites as they affect both the empty carrier and  $\text{Na}^+$  binding partial reactions.<sup>91,98</sup>

How fast does NaPi-IIa transport? Using steady-state and presteady-state electrophysiological data, the turnover rate of NaPi-II proteins has been recently compared for several isoforms.<sup>100</sup> The data suggest rates in the range  $4\text{--}10\text{ s}^{-1}$  at  $20^\circ\text{C}$ . As the NaPi-IIa kinetics are strongly temperature dependent (I.C. Forster, A. Bacconi unpublished data), we would expect values at least threefold higher under normal physiological conditions.

#### Probing NaPi-II proteins for structure–function relationships

Structure–function studies are used to identify molecular elements responsible for the observed transport characteristics, for example, substrate binding/interaction sites, voltage-sensing elements, and transport pathways etc. These studies can also yield topological and conformation information. Typically, these approaches rely on site-directed mutagenesis, covalent linking of reporter probes at specific sites and engineering chimeras derived from isoforms with different kinetic characteristics.

We have applied the substituted cysteine accessibility method<sup>101</sup> to probe the NaPi-IIa protein for functionally important sites.<sup>69–74</sup> substituted cysteine accessibility method involves replacing amino acids individually by cysteines and then probing the mutant with cysteine-reactive methanethio-sulfonate (MTS) reagents. Surface labeling of accessible cysteines can be confirmed by immunohistochemistry using MTS-biotin, and if the transport function is also modified, the accessibility of the site using different MTS reagents (size and charge) can be quantified (for review, see Forster *et al.*<sup>92</sup>). We first used substituted cysteine accessibility method to investigate the loops that link predicted membrane spanning regions<sup>69–71,73,74</sup> and thus confirmed their membrane orientation. Scanning of the predicted transmembrane spanning domain 5 (Figure 4a) indicated that this region is most likely inaccessible from the external medium and that it contains residues possibly involved in coordinating  $\text{Na}^+$  ions.<sup>72</sup> An

$\alpha$ -helical region was proposed from the periodical accessibility of sites in part of the second reentrant motif (Figure 4a, 9), consistent with the predictions of a hidden Markov analysis of the NaPi-IIa primary sequence.<sup>67</sup> Cysteine substitution in the linker stretches between domains 1, 2 and 11, 12 markedly affected the voltage dependency of the cotransport mode and this behavior suggested that the preferred orientation of the empty carrier (inward or outward facing) may be influenced by the flexibility of these linker stretches.<sup>73,74</sup>

The cloning of an electroneutral  $\text{Na}^+$ -coupled  $\text{P}_i$  cotransporter (NaPi-IIc),<sup>4</sup> which shows a high degree of sequence similarity to the electrogenic NaPi-IIa, particularly in the predicted membrane spanning regions, offered a unique opportunity to gain new insight into the NaPi-II transport mechanism. We first established that NaPi-IIc cotransports with a 2:1  $\text{Na}^+:\text{P}_i$  stoichiometry, consistent with its electroneutrality. Then, by means of a combination of engineering chimeras between each isoform, detailed sequence comparison, and site-directed mutagenesis, we identified conserved sites in each isoform that are critical for conferring electrogenicity (Figure 4a).<sup>5,72</sup> Substitution of three amino acids found at the equivalent sites in NaPi-IIa (see Figure 4a) conferred electrogenic behavior, including 3:1  $\text{Na}^+:\text{P}_i$  stoichiometry, to the electroneutral NaPi-IIc and, moreover, robust presteady-state relaxations were documented. Significantly, this finding demonstrated that relatively minor changes to the amino-acid sequence could establish a novel  $\text{Na}^+$  binding site and a concomitant change of the cotransport stoichiometry. Such molecular engineering does not come without a price: the electrogenic NaPi-IIc mutant exhibits a significantly reduced affinity for  $\text{P}_i$  compared with the WT NaPi-IIc (and NaPi-IIa) and a weaker dependency on membrane potential. These modified characteristics clearly indicate that other sites contribute to the kinetic fingerprint of NaPi-IIa.

The complexity and duplicity of structure–function relationships is also exemplified by our finding that similar

alterations in a macroscopic kinetic property can be effected by changes at different sites in the protein: for example, substituting a cysteine for a serine at the top of  $\alpha$ -helical region 9 (Figure 4a), leaves the electrogenic behavior essentially unchanged.<sup>69</sup> Modification of this site using MTS reagents fully inhibits cotransport activity, but retains the leak. Yet, exactly the same phenotype can be observed by simply replacing a native asparagine in  $\alpha$ -helical region 4 (Figure 4a) with charged or bulkier amino acids.<sup>71</sup> This may suggest an interaction of these two regions with the transport pathway, but does not exclude other explanations.

Recently the application of VCF (e.g. Cha *et al.*<sup>102</sup>), has revealed new structure–function relations of the NaPi-II protein. VCF combines electrophysiology and fluorescence microscopy, whereby specific sites of the protein are labeled with a fluorophore to report changes in the fluorophore's local environment in real-time under voltage clamp. One advantage of VCF is its potential to reveal local conformational changes, in contrast to presteady-state charge movements that may reflect global changes because the mobile charges could be distributed throughout the protein. In the first application of VCF to NaPi-II proteins, we used a mutant NaPi-II that shows no cotransport activity after MTS labeling,<sup>69</sup> yet, electrophysiological evidence indicates that substrates can still interact with the protein. This property implies that the number of possible conformational states (Figure 5d) is reduced, thus making data interpretation easier. The dependency of the fluorescence changes with external  $\text{Na}^+$  indicated that two  $\text{Na}^+$  ions can interact with the protein before  $\text{P}_i$  binding (Figure 5d) and that  $\text{Li}^+$  ions, which do not support cotransport, also interact with the first  $\text{Na}^+$  binding reaction.<sup>99</sup> In another VCF study, we have recorded fluorescence changes independently from four labeled sites located in externally accessible linker regions. Importantly, the labeling of these sites did not significantly alter cotransport function.<sup>103</sup> The dependency of fluorescence changes on substrate and membrane potential indicated that complementary conformational changes take place during the transport cycle in the two halves of the protein, when measured from their respective local environments. These VCF studies offer a first glimpse of the molecular rearrangements taking place at specific sites during substrate interaction and translocation in real time.

## OUTLOOK

At the physiological level, we still do not fully understand many aspects of renal phosphate handling. Recent evidence that NaPi-IIc cotransporters may (in humans) play a more important role than expected<sup>9</sup> will necessitate more detailed studies at the whole animal and at the cellular levels. Adaptation of renal  $\text{P}_i$  handling in response to changing dietary  $\text{P}_i$  is a well-documented phenomenon, yet the systemic and local signaling pathways remain to be elucidated. From the systemic viewpoint, one might hypothesize that a  $\text{P}_i$  sensor is involved, which would require identification. Recently, tantalizing evidence has emerged

from experiments that suggest that the  $\text{P}_i$  concentration in the third ventricle may influence the abundance of NaPi-IIa cotransporters.<sup>104</sup> Whether or not this is achieved via a neural pathway remains to be determined. On the other hand, alterations of blood  $\text{P}_i$  may provoke yet unknown hormonal responses that lead to changes in gene transcription or influence translation in the proximal tubular epithelia. Hormonal influences on the abundance of NaPi-IIa protein in the proximal tubular apical membrane are well described, yet in most cases we still do not understand the signaling mechanism that earmarks the protein for internalization, the phosphorylation reactions involved, whether or not the abundance of NaPi-II protein is indirectly affected by interacting proteins and the rate of endocytosis. Finally, the mechanism of apical sorting and targeting of type II  $\text{Na}^+/\text{P}_i$  cotransporters to the membrane remains to be elucidated.

At the molecular level, structural information as obtained from two- or three-dimensional crystallization of the NaPi-II protein will be essential to fully understand its transport mechanism, identify substrate coordination sites, the transmembrane transport pathway and resolve mechanistic issues concerning the nature of the carrier versus channel-like behavior this protein. This will complement our ongoing efforts to determine structure–function relationships using indirect biochemical and biophysical methods as described above. Furthermore, basic kinetic studies will also be required to elucidate the internal steps of the transport pathway by gaining access to the intracellular milieu. We should emphasize that this review has concentrated on what is known about the movement of  $\text{P}_i$  across the apical membrane of proximal tubule cells. Yet, it is obvious that an essential link in the overall movement of  $\text{P}_i$  from glomerular filtrate to blood still remains undefined, namely the mechanism and identification of the proteins responsible for basolateral exit of  $\text{P}_i$ .

## ACKNOWLEDGMENTS

We acknowledge the valuable contributions made by past and present members of our group. We thank Dr LV Virkki for insightful comments on this paper. This work was supported by the Swiss National Science Foundation, the Gebert R f Foundation, and Transregio SFB 11-Konstanz-Z rich.

## REFERENCES

1. Murer H, Forster I, Biber J. The sodium phosphate cotransporter family SLC34. *Pflugers Arch* 2004; **447**: 763–767.
2. Barac-Nieto M, Alfred M, Spitzer A. Basolateral phosphate transport in renal proximal-tubule-like OK cells. *Exp Biol Med* 2002; **227**: 626–631.
3. Forster IC, Loo DD, Eskandari S. Stoichiometry and  $\text{Na}^+$  binding cooperativity of rat and flounder renal type II  $\text{Na}^+/\text{P}_i$  cotransporters. *Am J Physiol* 1999; **276**: F644–F649.
4. Segawa H, Kaneko I, Takahashi A *et al.* Growth-related renal type II Na/Pi cotransporter. *J Biol Chem* 2002; **277**: 19665–19672.
5. Bacconi A, Virkki LV, Biber J *et al.* Renouncing electroneutrality is not free of charge: switching on electrogenicity in a  $\text{Na}^+$ -coupled phosphate cotransporter. *Proc Natl Acad Sci USA* 2005; **102**: 12606–12611.
6. Beck L, Karaplis AC, Amizuka N *et al.* Targeted inactivation of Npt2 in mice leads to severe renal phosphate wasting, hypercalciuria, and skeletal abnormalities. *Proc Natl Acad Sci USA* 1998; **95**: 5372–5377.
7. Levi M, Lotscher M, Sorribas V *et al.* Cellular mechanisms of acute and chronic adaptation of rat renal  $\text{P}_i$  transporter to alterations in dietary  $\text{P}_i$ . *Am J Physiol* 1994; **267**: F900–F908.

8. Keusch I, Traebert M, Lotscher M *et al.* Parathyroid hormone and dietary phosphate provoke a lysosomal routing of the proximal tubular Na<sup>+</sup>/P<sub>i</sub>-cotransporter type II. *Kidney Int* 1998; **54**: 1224–1232.
9. Segawa H, Yamanaka S, Ito M *et al.* Internalization of renal type IIc Na<sup>+</sup>/P<sub>i</sub>-cotransporter in response to a high-phosphate diet. *Am J Physiol Renal Physiol* 2005; **288**: F587–F596.
10. Murer H, Hernando N, Forster I, Biber J. Regulation of Na<sup>+</sup>/P<sub>i</sub> transporter in the proximal tubule. *Annu Rev Physiol* 2003; **65**: 531–542.
11. Lotscher M, Kaissling B, Biber J *et al.* Role of microtubules in the rapid regulation of renal phosphate transport in response to acute alterations in dietary phosphate content. *J Clin Invest* 1997; **99**: 1302–1312.
12. Pfister MF, Hilfiker H, Forgo J *et al.* Cellular mechanisms involved in the acute adaptation of OK cell Na<sup>+</sup>/P<sub>i</sub>-cotransport to high- or low-P<sub>i</sub> medium. *Pflugers Arch* 1998; **435**: 713–719.
13. Weinman EJ, Boddeti A, Cunningham R *et al.* NHERF-1 is required for renal adaptation to a low-phosphate diet. *Am J Physiol Renal Physiol* 2003; **285**: F1225–F1232.
14. Pfister MF, Lederer E, Forgo J *et al.* Parathyroid hormone-dependent degradation of type II Na<sup>+</sup>/P<sub>i</sub> cotransporters. *J Biol Chem* 1997; **272**: 20125–20130.
15. Karim-Jimenez Z, Hernando N, Biber J, Murer H. Molecular determinants for apical expression of the renal type IIa Na<sup>+</sup>/P<sub>i</sub>-cotransporter. *Pflugers Arch* 2001; **442**: 782–790.
16. Gisler SM, Stagljar I, Traebert M *et al.* Interaction of the type IIa Na<sup>+</sup>/P<sub>i</sub> cotransporter with PDZ proteins. *J Biol Chem* 2001; **276**: 9206–9213.
17. McWilliams RR, Breusegem SY, Brodsky KF *et al.* Shank2E binds Na<sup>+</sup>/P<sub>i</sub> cotransporter at the apical membrane of proximal tubule cells. *Am J Physiol Cell Physiol* 2005; **289**: C1042–C1051.
18. Noury C, Grant SG, Borg JP. PDZ domain proteins: plug and play! *Sci STKE* 2003; **179**: RE7.
19. Weinman EJ, Steplock D, Wang Y, Shenolikar S. Characterization of a protein cofactor that mediates protein kinase A regulation of the renal brush border membrane Na<sup>+</sup>-H<sup>+</sup> exchanger. *J Clin Invest* 1995; **95**: 2143–2149.
20. Yun CH, Lamprecht G, Forster DV, Sidor A. NHE3 kinase A regulatory protein E3KARP binds the epithelial brush border Na<sup>+</sup>/H<sup>+</sup> exchanger NHE3 and the cytoskeletal protein ezrin. *J Biol Chem* 1998; **273**: 25856–25863.
21. Murthy A, Gonzalez-Agosti C, Cordero E *et al.* NHE-RF, a regulatory cofactor for Na<sup>+</sup>-H<sup>+</sup> exchange, is a common interactor for merlin and ERM (MERM) proteins. *J Biol Chem* 1998; **273**: 1273–1276.
22. Wade JB, Liu J, Coleman RA *et al.* Localization and interaction of NHERF isoforms in the renal proximal tubule of the mouse. *Am J Physiol Cell Physiol* 2003; **285**: C1494–C1503.
23. Hernando N, Deliot N, Gisler SM *et al.* PDZ-domain interactions and apical expression of type IIa Na<sup>+</sup>/P<sub>i</sub> cotransporters. *Proc Natl Acad Sci USA* 2002; **99**: 11957–11962.
24. Shenolikar S, Voltz JW, Minkoff CM *et al.* Targeted disruption of the mouse NHERF-1 gene promotes internalization of proximal tubule sodium-phosphate cotransporter type IIa and renal phosphate wasting. *Proc Natl Acad Sci USA* 2002; **99**: 11470–11475.
25. Weinman EJ, Mohanlal V, Stoycheff N *et al.* Longitudinal study of urinary excretion of phosphate, calcium, and uric acid in mutant NHERF-1 null mice. *Am J Physiol Renal Physiol* 2006; **290**: F838–F843.
26. Kocher O, Comella N, Gilchrist A *et al.* PDZK1, a novel PDZ domain-containing protein up-regulated in carcinomas and mapped to chromosome 1q21, interacts with cMOAT (MRP2), the multidrug resistance-associated protein. *Lab Invest* 1999; **79**: 1161–1170.
27. Capuano P, Bacic D, Stange G *et al.* Expression and regulation of the renal Na<sup>+</sup>/phosphate cotransporter NaPi-IIa in a mouse model deficient for the PDZ protein PDZK1. *Pflugers Arch* 2005; **449**: 392–402.
28. Boeckers TM, Bockmann J, Kreutz MR, Gundelfinger ED. ProSAP/Shank proteins – a family of higher order organizing molecules of the postsynaptic density with an emerging role in human neurological disease. *J Neurochem* 2002; **81**: 903–910.
29. Okamoto PM, Gamby C, Wells D *et al.* Dynamin isoform-specific interaction with the shank/ProSAP scaffolding proteins of the postsynaptic density and actin cytoskeleton. *J Biol Chem* 2001; **276**: 48458–48465.
30. De Camilli P, Takei K, McPherson PS. The function of dynamin in endocytosis. *Curr Opin Neurobiol* 1995; **5**: 559–565.
31. Traebert M, Volk H, Biber J *et al.* Luminal and contraluminal action of 1–34 and 3–34 PTH peptides on renal type IIa Na<sup>+</sup>/P<sub>i</sub> cotransporter. *Am J Physiol Renal Physiol* 2000; **278**: F792–F798.
32. Mahon MJ, Donowitz M, Yun CC, Segre GV. Na<sup>+</sup>/H<sup>+</sup> exchanger regulatory factor 2 directs parathyroid hormone 1 receptor signalling. *Nature* 2002; **417**: 858–861.
33. Capuano P, Bacic D, Roos M *et al.* Defective coupling of apical PTH-receptors to phospholipase C prevents internalization of the Na<sup>+</sup>/phosphate cotransporter NaPi-IIa in NHERF1 deficient mice. *Am J Physiol-Renal* 2006 (in press).
34. Bacic D, Schulz N, Biber J *et al.* Involvement of the MAPK-kinase pathway in the PTH-mediated regulation of the proximal tubule type IIa Na<sup>+</sup>/P<sub>i</sub> cotransporter in mouse kidney. *Pflugers Arch* 2003; **446**: 52–60.
35. Weinman EJ, Cunningham R, Shenolikar S. NHERF and regulation of the renal sodium-hydrogen exchanger NHE3. *Pflugers Arch* 2005; **450**: 137–144.
36. Collazo R, Fan L, Hu MC *et al.* Acute regulation of Na<sup>+</sup>/H<sup>+</sup> exchanger NHE3 by parathyroid hormone via NHE3 phosphorylation and dynamin-dependent endocytosis. *J Biol Chem* 2000; **275**: 31601–31608.
37. Honegger KJ, Capuano P, Winter C *et al.* Regulation of sodium-proton exchanger isoform 3 (NHE3) by PKA and exchange protein directly activated by cAMP (EPAC). *Proc Natl Acad Sci USA* 2006; **103**: 803–808.
38. Traebert M, Roth J, Biber J *et al.* Internalization of proximal tubular type II Na<sup>+</sup>-P<sub>i</sub> cotransporter by PTH: immunogold electron microscopy. *Am J Physiol Renal Physiol* 2000; **278**: F148–F154.
39. Yang LE, Maunsbach AB, Leong PK, McDonough AA. Differential traffic of proximal tubule Na<sup>+</sup> transporters during hypertension or PTH: NHE3 to base of microvilli vs. NaPi2 to endosomes. *Am J Physiol Renal Physiol* 2004; **287**: F896–F906.
40. Bacic D, Lehir M, Biber J *et al.* The renal Na<sup>+</sup>/phosphate cotransporter NaPi-IIa is internalized via the receptor-mediated endocytic route in response to parathyroid hormone. *Kidney Int* 2006; **69**: 495–503.
41. Bacic D, Capuano P, Gisler SM *et al.* Impaired PTH-induced endocytotic down-regulation of the renal type IIa Na<sup>+</sup>/P<sub>i</sub>-cotransporter in RAP-deficient mice with reduced megalin expression. *Pflugers Arch* 2003; **446**: 475–484.
42. Lotscher M, Scarpetta Y, Levi M *et al.* Rapid downregulation of rat renal Na<sup>+</sup>/P<sub>i</sub> cotransporter in response to parathyroid hormone involves microtubule rearrangement. *J Clin Invest* 1999; **104**: 483–494.
43. Robinson MS. Adaptable adaptors for coated vesicles. *Trends Cell Biol* 2004; **14**: 167–174.
44. Hernando N, Forgo J, Biber J, Murer H. PTH-induced downregulation of the type IIa Na<sup>+</sup>/P<sub>i</sub>-cotransporter is independent of known endocytic motifs. *J Am Soc Nephrol* 2000; **11**: 1961–1968.
45. Karim-Jimenez Z, Hernando N, Biber J *et al.* A dibasic motif involved in parathyroid hormone-induced down-regulation of the type IIa NaPi cotransporter. *Proc Natl Acad Sci USA* 2000; **97**: 12896–12901.
46. Ito M, Iidawa S, Izuka M *et al.* Interaction of a farnesylated protein with renal type IIa Na<sup>+</sup>/P<sub>i</sub> co-transporter in response to parathyroid hormone and dietary phosphate. *Biochem J* 2004; **377**: 607–616.
47. Deliot N, Hernando N, Horst-Liu Z *et al.* Parathyroid hormone treatment induces dissociation of type IIa Na<sup>+</sup>-Pi cotransporter-Na<sup>+</sup>/H<sup>+</sup> exchanger regulatory factor-1 complexes. *Am J Physiol Cell Physiol* 2005; **289**: C159–C167.
48. Hall RA, Spurney RF, Premont RT *et al.* G protein-coupled receptor kinase 6A phosphorylates the Na<sup>+</sup>/H<sup>+</sup> exchanger regulatory factor via a PDZ domain-mediated interaction. *J Biol Chem* 1999; **274**: 24328–24334.
49. He J, Lau AG, Yaffe MB, Hall RA. Phosphorylation and cell cycle-dependent regulation of Na<sup>+</sup>/H<sup>+</sup> exchanger regulatory factor-1 by Cdc2 kinase. *J Biol Chem* 2001; **276**: 41559–41565.
50. Raghuram V, Hormuth H, Foskett JK. A kinase-regulated mechanism controls CFTR channel gating by disrupting bivalent PDZ domain interactions. *Proc Natl Acad Sci USA* 2003; **100**: 9620–9625.
51. Nakamura T, Shibata N, Nishimoto-Shibata T *et al.* Regulation of SR-BI protein levels by phosphorylation of its associated protein, PDZK1. *Proc Natl Acad Sci USA* 2005; **102**: 13404–13409.
52. Tenenhouse HS, Murer H. Disorders of renal tubular phosphate transport. *J Am Soc Nephrol* 2003; **14**: 240–248.
53. Tenenhouse HS, Beck L. Renal Na<sup>+</sup>-phosphate cotransporter gene expression in X-linked Hyp and Gy mice. *Kidney Int* 1996; **49**: 1027–1032.
54. Tenenhouse HS, Martel J, Gauthier C *et al.* Differential effects of Npt2a gene ablation and X-linked Hyp mutation on renal expression of Npt2c. *Am J Physiol Renal Physiol* 2003; **285**: F1271–F1278.
55. Francis F, Hennig S, Korn B *et al.* A gene (PEX) with homologies to endopeptidases is mutated in patients with X-linked hypophosphatemic rickets. The HYP Consortium. *Nat Genet* 1995; **11**: 130–136.
56. White KE, Evans WE, O'Riordan JH *et al.* Autosomal dominant hypophosphatemic rickets is associated with mutations in FGF23. *Nat Genet* 2000; **26**: 345–348.

57. Shimada T, Hasegawa H, Yamazaki Y *et al.* FGF-23 is a potent regulator of vitamin D metabolism and phosphate homeostasis. *J Bone Miner Res* 2004; **19**: 429–435.
58. Baum M, Schiavi S, Dwarakanath V, Quigley R. Effect of fibroblast growth factor-23 on phosphate transport in proximal tubules. *Kidney Int* 2005; **68**: 1148–1153.
59. Shimada T, Urakawa I, Yamazaki Y *et al.* FGF-23 transgenic mice demonstrate hypophosphatemic rickets with reduced expression of sodium phosphate cotransporter type IIa. *Biochem Biophys Res Commun* 2004; **314**: 409–414.
60. Tieder M, Modai D, Samuel R *et al.* Hereditary hypophosphatemic rickets with hypercalciuria. *N Engl J Med* 1985; **312**: 611–617.
61. Jones A, Tzenova J, Frappier D *et al.* Hereditary hypophosphatemic rickets with hypercalciuria is not caused by mutations in the Na/P<sub>i</sub> cotransporter NPT2 gene. *J Am Soc Nephrol* 2001; **12**: 507–514.
62. Prie D, Huart V, Bakouh N *et al.* Nephrolithiasis and osteoporosis associated with hypophosphatemia caused by mutations in the type 2a sodium-phosphate cotransporter. *N Engl J Med* 2002; **347**: 983–991.
63. Virkki LV, Forster IC, Hernando N *et al.* Functional characterization of two naturally occurring mutations in the human sodium-phosphate cotransporter type IIa. *J Bone Miner Res* 2003; **18**: 2135–2141.
64. Lorenz-Depiereux B, Benet-Pages A, Eckstein G *et al.* Hereditary hypophosphatemic rickets with hypercalciuria is caused by mutations in the sodium-phosphate cotransporter gene SLC34A3. *Am J Hum Genet* 2006; **78**: 193–201.
65. Bergwitz C, Roslin NM, Tieder M *et al.* SLC34A3 mutations in patients with hereditary hypophosphatemic rickets with hypercalciuria predict a key role for the sodium-phosphate cotransporter NaPi-IIc in maintaining phosphate homeostasis. *Am J Hum Genet* 2006; **78**: 179–192.
66. Murer H, Hernando N, Forster I, Biber J. Proximal tubular phosphate reabsorption: molecular mechanisms. *Physiol Rev* 2000; **80**: 1373–1409.
67. Radanovic T, Gisler SM, Murer H, Biber J. Topology of the type IIa Na<sup>+</sup>/P<sub>i</sub>-cotransporter. *J Membr Biol* 2006.
68. Lambert G, Traebert M, Hernando N *et al.* Studies on the topology of the renal type II NaPi-cotransporter. *Pflügers Archiv Eur J Physiol* 1999; **437**: 972–978.
69. Lambert G, Forster IC, Stange G *et al.* Properties of the mutant Ser-460-Cys implicate this site in a functionally important region of the type IIa Na<sup>+</sup>/P<sub>i</sub> cotransporter protein. *J Gen Physiol* 1999; **114**: 637–652.
70. Lambert G, Forster IC, Stange G *et al.* Cysteine mutagenesis reveals novel structure-function features within the predicted third extracellular loop of the type IIa Na<sup>+</sup>/P<sub>i</sub> cotransporter. *J Gen Physiol* 2001; **117**: 533–546.
71. Kohler K, Forster IC, Stange G *et al.* Identification of functionally important sites in the first intracellular loop of the NaPi-IIa cotransporter. *Am J Physiol* 2002; **282**: F687–F696.
72. Virkki LV, Forster IC, Bacconi A *et al.* Functionally important residues in the predicted 3rd transmembrane domain of the type IIa sodium-phosphate co-transporter (NaPi-IIa). *J Membr Biol* 2005; **206**: 227–238.
73. Ehnes C, Forster IC, Bacconi A *et al.* Structure-function relations of the first and fourth extracellular linkers of the type IIa Na<sup>+</sup>/P<sub>i</sub> cotransporter: II. Substrate interaction and voltage dependency of two functionally important sites. *J Gen Physiol* 2004; **124**: 489–503.
74. Ehnes C, Forster IC, Kohler K *et al.* Structure-function relations of the first and fourth predicted extracellular linkers of the type IIa Na<sup>+</sup>/P<sub>i</sub> cotransporter: I. Cysteine scanning mutagenesis. *J Gen Physiol* 2004; **124**: 475–488.
75. Kohler K, Forster IC, Stange G *et al.* Transport function of the renal type IIa Na<sup>+</sup>/P<sub>i</sub> cotransporter is codetermined by residues in two opposing linker regions. *J Gen Physiol* 2002; **120**: 693–703.
76. Lambert G, Forster IC, Biber J, Murer H. Cysteine residues and the structure of the rat renal proximal tubular type II sodium phosphate cotransporter (rat NaPi IIa). *J Membr Biol* 2000; **176**: 133–141.
77. Werner A, Kinne RK. Evolution of the Na-P<sub>i</sub> cotransport systems. *Am J Physiol – Regulat Integrat Comparat Physiol* 2001; **280**: R301–R312.
78. Kohl B, Wagner CA, Huelseweh B *et al.* The Na<sup>+</sup>-phosphate cotransport system (NaPi-II) with a cleaved protein backbone: implications on function and membrane insertion. *J Physiol* 1998; **508**: 341–350.
79. Kohler K, Forster IC, Stange G *et al.* Essential cysteine residues of the type IIa Na<sup>+</sup>/P<sub>i</sub> cotransporter. *Pflügers Archiv – Eur J Physiol* 2003; **446**: 203–210.
80. Doyle DA, Morais Cabral J, Pfuetzner RA *et al.* The structure of the potassium channel: molecular basis of K<sup>+</sup> conduction and selectivity. *Science* 1998; **280**: 69–77.
81. Dutzler R, Campbell EB, Cadene M *et al.* X-ray structure of a ClC chloride channel at 3.0 Å reveals the molecular basis of anion selectivity. *Nature* 2002; **415**: 287–294.
82. Kilic F, Rudnick G. Oligomerization of serotonin transporter and its functional consequences. *Proc Natl Acad Sci USA* 2000; **97**: 3106–3111.
83. Eskandari S, Kreman M, Kavanaugh MP *et al.* Pentameric assembly of a neuronal glutamate transporter. *Proc Natl Acad Sci USA* 2000; **97**: 8641–8646.
84. Yernool D, Boudker O, Jin Y, Gouaux E. Structure of a glutamate transporter homologue from *Pyrococcus horikoshii* (see comment). *Nature* 2004; **431**: 811–818.
85. Kohler K, Forster IC, Lambert G *et al.* The functional unit of the renal type IIa Na<sup>+</sup>/P<sub>i</sub> cotransporter is a monomer. *J Biol Chem* 2000; **275**: 26113–26120.
86. Eskandari S, Wright EM, Kreman M *et al.* Structural analysis of cloned plasma membrane proteins by freeze-fracture electron microscopy. *Proc Natl Acad Sci USA* 1998; **95**: 11235–11240.
87. Gisler SM, Fuster D, Radanovic T *et al.* Application of the type II split-ubiquitin membrane yeast two-hybrid system using whole epithelial transmembrane proteins as baits. 2006.
88. Busch A, Waldegger S, Herzer T *et al.* Electrophysiological analysis of Na<sup>+</sup>/P<sub>i</sub> cotransport mediated by a transporter cloned from rat kidney and expressed in *Xenopus* oocytes. *Proc Natl Acad Sci USA* 1994; **91**: 8205–8208.
89. Busch AE, Wagner CA, Schuster A *et al.* Properties of electrogenic P<sub>i</sub> transport by a human renal brush border Na<sup>+</sup>/P<sub>i</sub> transporter. *J Am Soc Nephrol* 1995; **6**: 1547–1551.
90. Hartmann CM, Wagner CA, Busch AE *et al.* Transport characteristics of a murine renal Na/P<sub>i</sub>-cotransporter (erratum appears in Pflügers Arch 1996 May;432(1):158). *Pflügers Archiv Eur J Physiol* 1995; **430**: 830–836.
91. Virkki LV, Forster IC, Biber J, Murer H. Substrate interactions in the human type IIa sodium-phosphate cotransporter (NaPi-IIa). *Am J Physiol – Renal Physiol* 2005; **288**: F969–F981.
92. Forster IC, Kohler K, Biber J, Murer H. Forging the link between structure and function of electrogenic cotransporters: the renal type IIa Na<sup>+</sup>/P<sub>i</sub> cotransporter as a case study. *Prog Biophys Mol Biol* 2002; **80**: 69–108.
93. Bezanilla F. Voltage-gated ion channels. *IEEE Trans Nanobiosci* 2005; **4**: 34–48.
94. DeFelix LJ. Transporter structure and mechanism. *Trends Neurosci* 2004; **27**: 352–359.
95. Accardi A, Miller C. Secondary active transport mediated by a prokaryotic homologue of ClC Cl<sup>-</sup> channels. *Nature* 2004; **427**: 803–807.
96. Sonders MS, Amara SG. Channels in transporters. *Curr Opin Neurobiol* 1996; **6**: 294–302.
97. Forster I, Hernando N, Biber J, Murer H. The voltage dependence of a cloned mammalian renal type II Na<sup>+</sup>/P<sub>i</sub> cotransporter (NaPi-2). *J Gen Physiol* 1998; **112**: 1–18.
98. Forster IC, Biber J, Murer H. Proton-sensitive transitions of renal type II Na<sup>+</sup>-coupled phosphate cotransporter kinetics. *Biophys J* 2000; **79**: 215–230.
99. Virkki LV, Murer H, Forster IC. Voltage clamp fluorometric measurements on a type II Na<sup>+</sup>-coupled P<sub>i</sub> cotransporter: Shedding light on substrate binding order. *J Gen Physiol* 2006; **127**: 539–555.
100. Forster IC, Virkki LV, Bossi E *et al.* Electrogenic kinetics of a mammalian intestinal type IIb Na<sup>+</sup>/P<sub>i</sub>-cotransporter. *J Membr Biol* 2006.
101. Karlin A, Akabas MH. Substituted-cysteine accessibility method. *Methods Enzymol* 1998; **293**: 123–145.
102. Cha A, Zerangue N, Kavanaugh M, Bezanilla F. Fluorescence techniques for studying cloned channels and transporters expressed in *Xenopus* oocytes. *Methods Enzymol* 1998; **296**: 566–578.
103. Virkki LV, Murer H, Forster IC. Mapping conformational changes of a type IIb Na<sup>+</sup>/P<sub>i</sub> cotransporter by voltage clamp fluorometry. *J Biol Chem* 2006 (in press).
104. Mulrone SE, Woda CB, Halaihel N *et al.* Central control of renal sodium-phosphate (NaPi-2) transporters. *Am J Physiol – Renal Physiol* 2004; **286**: F647–F652.